Electronic Supplementary Material

Enhancement of photoactivity and cellular uptake of $(Bu_4N)_2[Mo_6I_8(CH_3COO)_6]$ complex by loading on porous MCM-41 support. Photodynamic studies as an anticancer agent

Cristina de la Torre,[a,b] *Raquel Gavara,*[c] *Alba García-Fernández* [a,b,e] *Maxim Mikhaylov,*[d] *Maxim N. Sokolov,*[d] *Juan F. Miravet,*[c] *Félix Sancenón,*[a,b,e,f] *Ramón Martínez-Máñez**[a,b,e,f] *and Francisco Galindo**[c]

[a] Instituto Interuniversitario de Investigación de Reconocimiento Molecular y Desarrollo Tecnológico (IDM), Unidad Mixta Universitat Politècnica de València - Universidad de Valencia, Departamento de Química Universitat Politècnica de València, Camino de Vera s/n, 46022, Valencia, Spain. E-mail: rmaez@qim.upv.es

[b] CIBER de Bioingeniería, Biomateriales y Nanomedicina (CIBER-BBN), Spain.

[c] Departamento de Química Inórganica y Orgánica, Universitat Jaume I, Av. Sos Baynat s/n, 12071, Castellón, Spain. E-mail: francisco.galindo@uji.es

[d] Nikolaev Institute of Inorganic Chemistry, Siberian Branch of the Russian Academy of Sciences 3 Acad. Lavrentiev Prosp., 630090 Novosibirsk, Russia.

[e] Unidad Mixta UPV-CIPF de Investigación en Mecanismos de Enfermedades y Nanomedicina, Universitat Politècnica de València, Centro de Investigación Príncipe Felipe, Valencia, Spain.

[f] Unidad Mixta de Investigación en Nanomedicina y Sensores. Universitat Politècnica de València, IIS La Fe, Valencia, Spain.

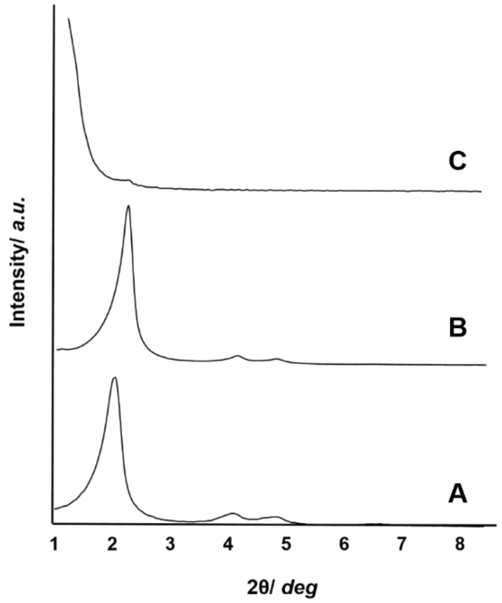

Figure S1. Powder X-ray diffraction pattern of **MCM-41** before calcination (a), calcined **MCM-41** (b) and final solid **1@MCM-41** (c) showing the typical reflections of the MSNs hexagonal array.

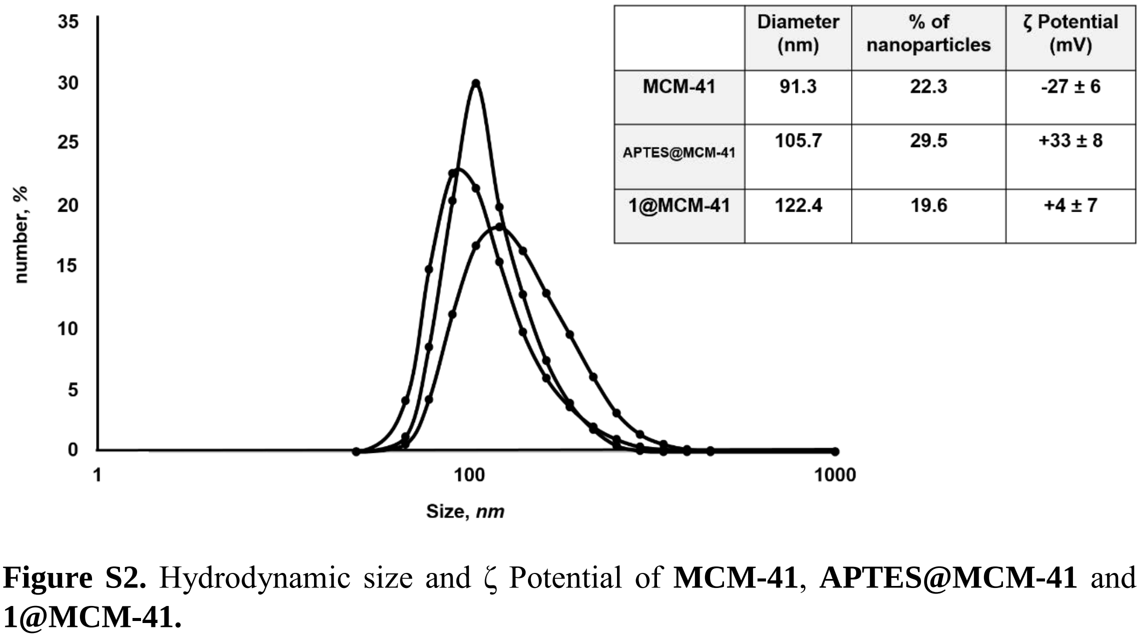

	Diameter (nm)	% of nanoparticles	ζ Potential (mV)
MCM-41	91.3	22.3	-27 ± 6
APTES@MCM-41	105.7	29.5	+33 ± 8
1@MCM-41	122.4	19.6	+4 ± 7

Figure S2. Hydrodynamic size and ζ Potential of **MCM-41**, **APTES@MCM-41** and **1@MCM-41.**

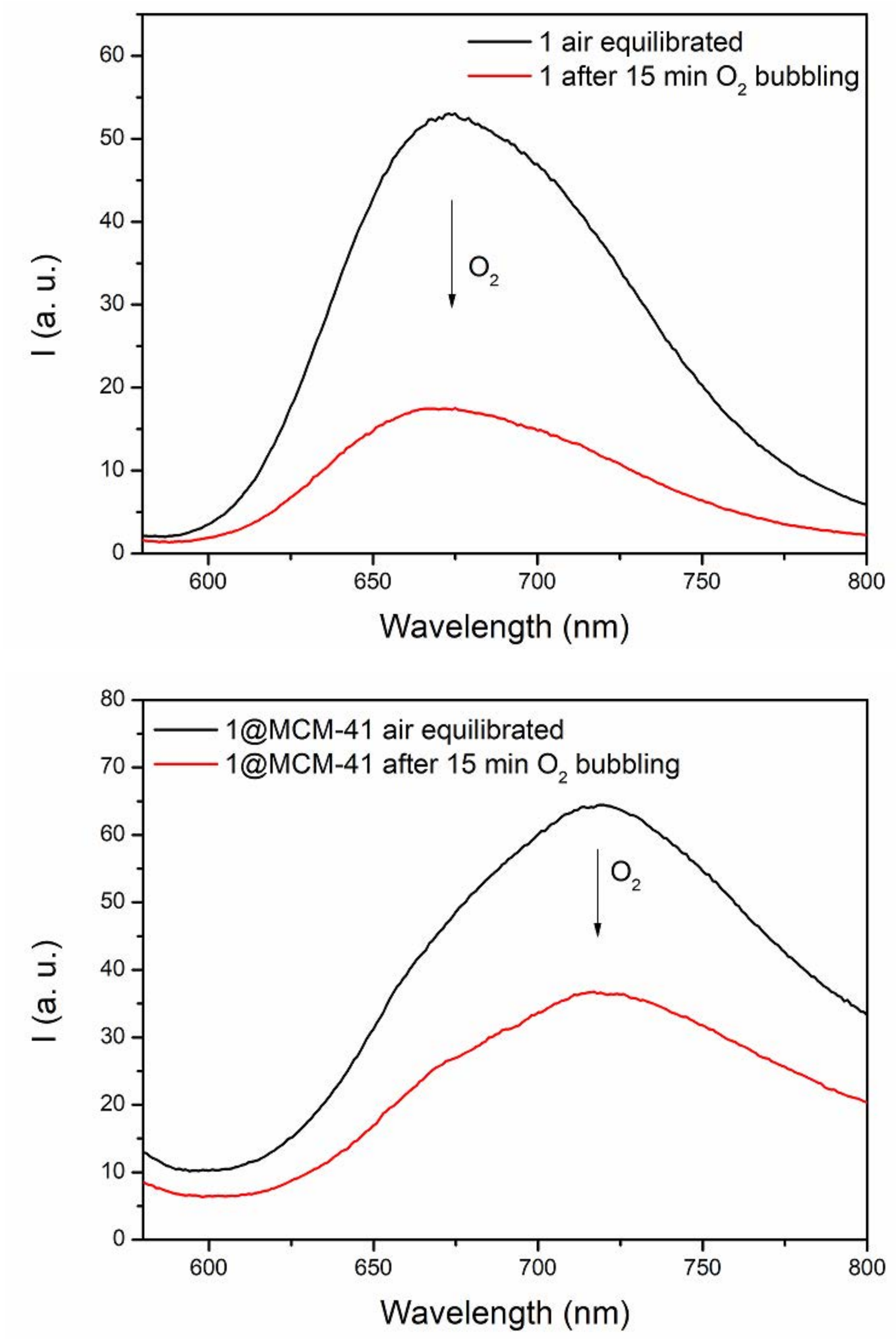

Figure S3. Up: Emission spectra corresponding to a solution of **1** (0.07 mg/mL) in water (10 mM PBS, pH = 7) air-equilibrated (black line) and after bubbling oxygen for 15 minutes (red line). Bottom: analogous spectra for **1@MCM-41** (0.1 mg/mL).

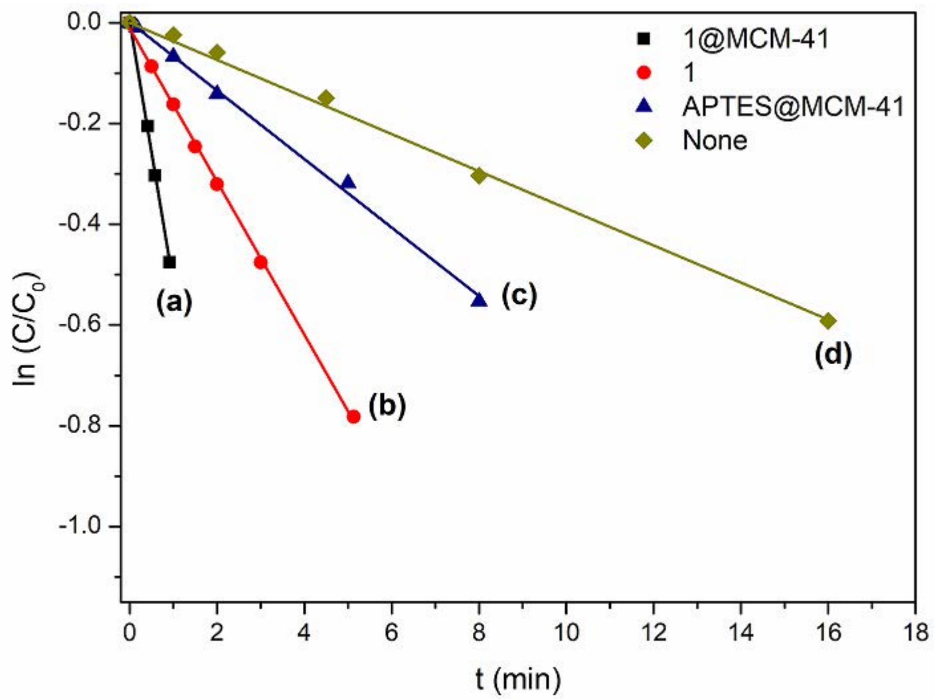

Figure S4. Pseudo-first order fittings ($\ln C/C_0$ vs. time) for the photooxidation reaction of ABDA (3.3×10^{-5} M) in water (PBS 10 mM, pH = 7) by: (a) **1@MCM-41** (0.1 mg mL^{-1}), (b) **1** (2.9×10^{-5} M), (c) **APTES@MCM-41** (0.1 mg mL^{-1}) and (d) autooxidation.

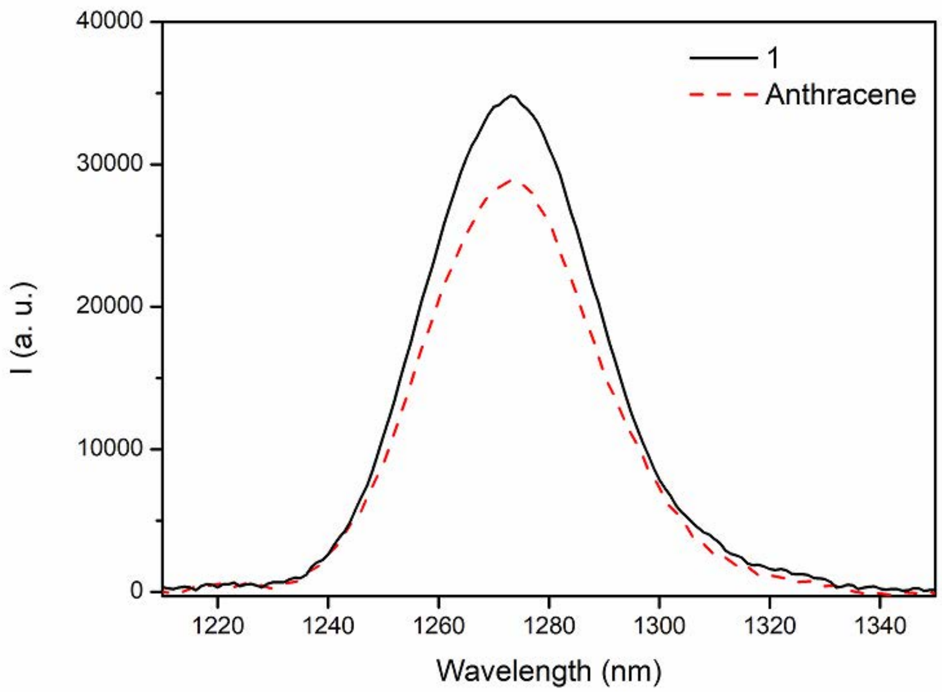

Figure S5. Singlet oxygen phosphorescence (λ_{exc} = 308 nm) recorded for oxygen saturated CH_3CN solutions of **1** (full line) and anthracene (dashed line). The quantum yield calculated for **1** is $\phi_\Delta = 0.86$.

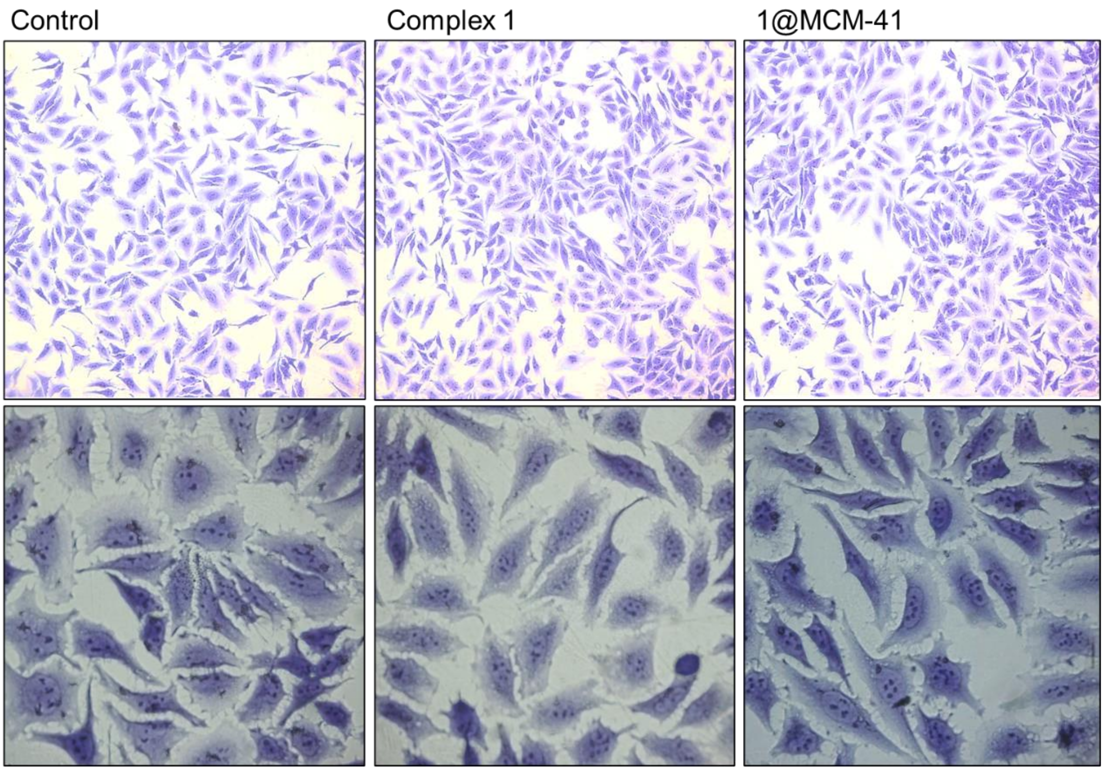

Figure S6. Crystal violet staining of HeLa cells in the presence of **1@MCM-41** and **1** complex at different magnifications 10X (up) and 40X (down).

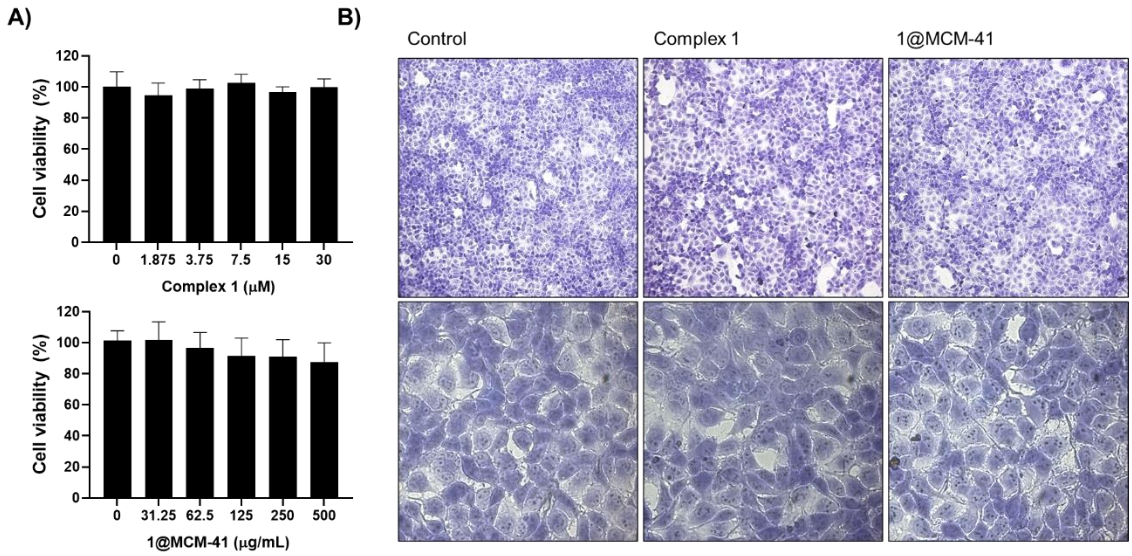

Figure S7. (A) Cell viability assays at different concentrations of complex **1** (up) and **1@MCM-41** nanoparticles (down) at 24h in SK-Mel-103 cells. Data represent the mean ± SEM of at least three independent experiments. (B) Crystal violet staining of SK-Mel-103 cells in the presence of **1@MCM-41** and **1** complex at different magnifications 10X (up) and 40X (down).

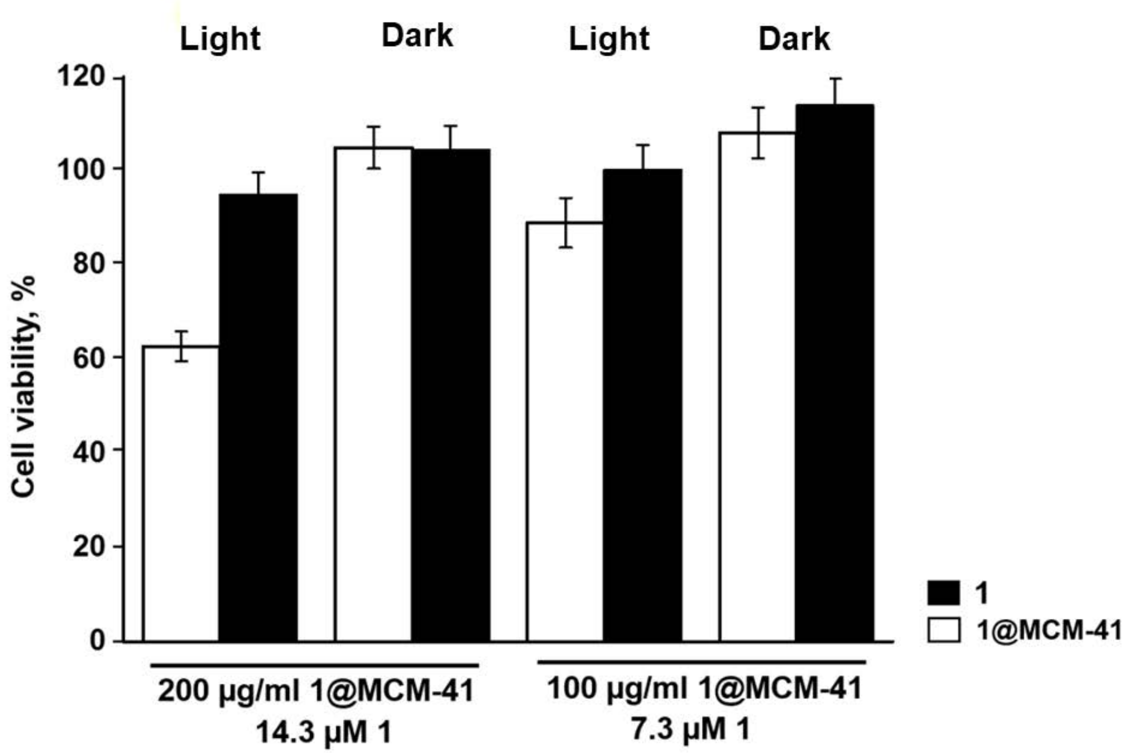

Figure S8. Toxicity and phototoxicity of **1@MCM-41** and **1** against Sk-mel cells.